Physics

Cole Memorial Library

SCIENCE OF LIGHT

VOLUME 6 NUMBER 3

December

1957

OHIO STATE UNIVERSITY
APR 24 1958
LIBRARY

Published by the

Institute for Optical Research

Tokyo University of Education

in collaboration with

The Spectroscopical Society of Japan

SCIENCE OF LIGHT

Science of Light contains reports of the Institute for Optical Research and contribution from other science bodies about similar subjects.

The editorial staff consists of following members:

Chairman: Prof. H. Ootsuka, *Tokyo University of Education*

Dr. Y. Fujioka, *Atomic Energy Commission of Japan*

Prof. E. Minami, *Tokyo University*

Prof. M. Seya, *Tokyo University of Education*

Prof. Y. Uchida, *Kyoto University*

Prof. T. Uemura, *Rikkyo University*

Prof. K. Miyake, *Tokyo University of Education*

All communications should be addressed to the director or to the librarian of the Institute.

The Institute for Optical Research

Tokyo University of Education

400, 4-chome, Hyakunin-machi, Shinjuku-ku, Tokyo, Japan

Printed at
the Printing Department, Chūō Kagakusha,
Tokyo

A Method of Calculating Interference Color of Thin Films Using an Automatic Relay Computer

Kazuo MIYAKE

Institute for Optical Research, Tokyo University of Education

Shinjuku-ku, Tokyo

(Received November 15, 1957)

Abstract

Using an automatic relay computer, a method for determining the interference color of thin films is studied. Calculation of chromaticity of the interference color is performed more conveniently by the summation of integrand at equal intervals of wavenumber than at equal intervals of wavelength, if the change of refractive index with wavelength is neglected.

The CIE colorimetric data of $E_\lambda\bar{x}_\lambda$, $E_\lambda\bar{y}_\lambda$, $E_\lambda\bar{z}_\lambda$ are transformed into a table using the wavenumber in 200 cm^{-1} intervals as variable and are given in the range extending from 13,000 cm^{-1} to 27,000 cm^{-1}.

1. Introduction

The colorimetric calculation, needed to determine the chromaticity of a color from its spectral intensity distribution, is rather laborious. Mechanical computers suited to this purpose have been designed and used. Computation of the interference color of thin films is much more tedious than that of ordinary color. A method to save the labor and simplify the theoretical interpretation of results has been adopted by neglecting the effect of multiply reflected rays[1)2)].

Lately, such high-speed automatic calculating machines as the electronic computer and the electric relay computer have been developed. It seems natural that much time and labor of above-mentioned computation will be saved by using these computers. An application of IBM electronic computer to colorimetric calculation has been reported[3)].

Pressed by the need of determining the interference color of stained glass surfaces coated with anti-reflecting films, an attempt has been made to apply an electric relay computer to this problem.

The computer FACOM-128, made by the Fuji Communication Apparatus MFG. Co., was used simply because it was easily accessible to the author, and

1) H. Kubota: J. Opt. Soc. Am. **40** (1950) 146.
2) H. Kubota: Rep. Inst. Indust. Sci. Tokyo Univ., **2** (1952) 205.
G. C. Monch: Optik **9** (1952) 97.
3) W. E. White and D. L. MacAdam: J. Opt. Soc. Am. **47** (1957) 605.

after all, it was found for the present most convenient as it has a large capacity of memorial elements. For calculation, the program of colorimetric procedure was devised to be easily applicable to the operation of the relay computer.

2. The Colorimetric Calculation Method

Description of the procedure adopted by the CIE Committee on Colorimetry to specify the chromaticity of a color[4] is here left out except on a few points considered necessary for explanation.

Let E_λ be the energy per unit width of wavelength in the distribution of the light source energy, R_λ the reflection coefficient of the surface under consideration for the light of wavelength λ, $\bar{x}_\lambda$, $\bar{y}_\lambda$, $\bar{z}_\lambda$ the tristimulus values of the spectrum color, X, Y, Z the tristimulus values of the reflected light, x, y, z the tristimulus coefficients of the reflected light, then the chromaticity of the reflected light is given as

$$X=\int E_\lambda \bar{x}_\lambda R_\lambda d\lambda, \quad Y=\int E_\lambda \bar{y}_\lambda R_\lambda d\lambda, \quad Z=\int E_\lambda \bar{z}_\lambda R_\lambda d\lambda \tag{1}$$

$$x=X/S, \quad y=Y/S, \quad z=Z/S$$

$$S=X+Y+Z \tag{2}$$

Usually, numerical calculations by summation are substituted for the integrations in (1). Although there are two ways to perform this calculation, that is, the selected ordinate method and the weighted ordinate method, the latter was used by the reason described below.

The reflection coefficient R_λ of a double layer is given by

$$R_\lambda=1-(1-r_0^2)(1-r_1^2)(1-r_2^2)/D$$

$$D=1+(r_0r_1)^2+(r_1r_2)^2+(r_2r_0)^2$$
$$+2\{r_1r_2(1+r_0^2)\cos\delta_2+r_0r_1(1+r_2^2)\cos\delta_1$$
$$+r_2r_0[\cos(\delta_1+\delta_2)+r_1^2\cos(\delta_1-\delta_2)]\} \tag{3}$$

where r_0, r_1, r_2 are the amplitude reflection coefficients of the boundary planes between mediums as shown in Fig. 1.

For the sake of simplicity, only the case of normal incidence will be considered hereafter. Let the refractive indices of the mediums be n_0, n_1, n_2, n_3 in ascending order from the bottom, we have the following relations,

---

4) Committee on Colorimetry: J. Opt. Soc. Am. **34** (1944) 633.
A. C. Hardy: *Handbook of Colorimetry*. (The Technology Press, M.I.T., Cambridge, 1936).

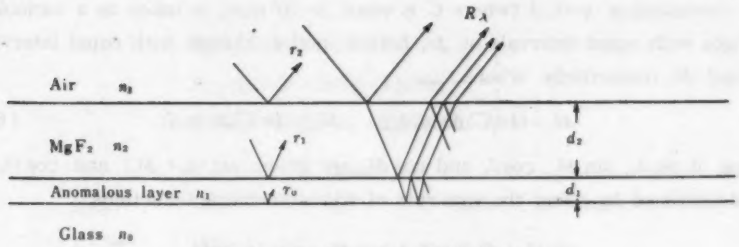

Fig. 1. Structure of a double layer

$$r_0=\frac{n_0-n_1}{n_0+n_1}\,,\qquad r_1=\frac{n_1-n_2}{n_1+n_2}\,,\qquad r_2=\frac{n_2-n_3}{n_2+n_3} \tag{4}$$

The phase angles in (3) are given as

$$\delta_1=(4\pi/\lambda)n_1d_1\,,\qquad \delta_2=(4\pi/\lambda)n_2d_2\,, \tag{5}$$

where d_1, d_2 are the thicknesses of the mediums 1 and 2. Let us use mμ as the unit of measure for wavelength and optical thickness of films.

If the interference color of this doubly layered surface is to be determined, firstly the reflection coefficient R_λ has to be calculated for the wavelengths, which are selected as the calculation points. Then, in the case of selected ordinate method, R_λs must be summed up for all the selected wavelengths to obtain the tristimulus values X, Y, Z. In the case of weighted ordinate method, the summation is to be performed after multiplying R_λs with $E_\lambda\bar{x}_\lambda$, $E_\lambda\bar{y}_\lambda$, $E_\lambda\bar{z}_\lambda$ of corresponding wavelengths as weighting factors. R_λ involves δ_1, δ_2 in the forms of $\cos\delta_1$, $\cos\delta_2$, $\cos(\delta_1+\delta_2)$, $\cos(\delta_1-\delta_2)$ as the expressions (3) show. When the computation is made with a hand operated calculating machine, numerical values of these functions are found in a trigonometric function table. But for the automatic calculating machine, they will have to be calculated separately. Using a calculator such as a relay computer, the speed of which is rather slow, not only it makes the programming troublesome but also the time of computation becomes so long that the advantage of using such an automatic computer will be countervailed.

In the selected ordinate method, the wavelengths of the calculation points are given in the intervals which are inversely proportional to the values of $E_\lambda\bar{x}_\lambda$, $E_\lambda\bar{y}_\lambda$, $E_\lambda\bar{z}_\lambda$ and therefore there is no simple rule to define their intervals. In the weighted ordinate method, they are given in equal intervals, for example, at every 10 mμ. As it is apparent from (5), δ_1 and δ_2 do not change in equal intervals even if λ changes with equal intervals. Neglecting the change of refractive indices n_1, n_2 with the wavelength, δ_1 and δ_2 become proportional to $1/\lambda$.

Therefore, if the quantity, which changes proportionally to $1/\lambda$, for example,

the wavenumber $\nu=C/\lambda$ (where C is equal to $10^5\,\mathrm{m}\mu$), is taken as a variable and changes with equal intervals of $\Delta\nu$, both δ_1 and δ_2 change with equal intervals of $\Delta\delta_1$ and $\Delta\delta_2$ respectively, where

$$\Delta\delta_1=(4\pi/C)\Delta\nu\cdot n_1d_1\,,\qquad \Delta\delta_2=(4\pi/C)\Delta\nu\cdot n_2d_2\,. \tag{6}$$

Hence, if $\sin\delta_1$, $\sin\Delta\delta_1$, $\cos\delta_1$ and $\cos\Delta\delta_1$ are given, $\sin(\delta_1+\Delta\delta_1)$ and $\cos(\delta_1+\Delta\delta_1)$ are determined by using the sum-rule of trigonometrical founctions

$$\left.\begin{aligned}\sin(\delta_1+\Delta\delta_1)&=\sin\delta_1\cos\Delta\delta_1+\cos\delta_1\sin\Delta\delta_1\\ \cos(\delta_1+\Delta\delta_1)&=\cos\delta_1\cos\Delta\delta_1-\sin\delta_1\sin\Delta\delta_1\end{aligned}\right\}. \tag{7}$$

Repeating this process, $\sin(\delta_1+m\Delta\delta_1)$ and $\cos(\delta_1+m\Delta\delta_1)$ are determined easily, where m is an integer.

As this process is of only arithmetical operations, there is no trouble in using an automatic computer, and the computation was performed on an automatic relay computer by the weighted ordinate method taking the wavenumber in equal intervals as the variable.

3. The Computation

The CIE colorimetric data give the numerical values of $E_\lambda\bar{x}_\lambda$, $E_\lambda\bar{y}_\lambda$, $E_\lambda\bar{z}_\lambda$ for the CIE A-, B- and C-Illuminants in $10\,\mathrm{m}\mu$ intervals. It is necessary to convert them into a form of tables with equal intervals of ν. At first, the values of $E_\lambda\bar{x}_\lambda$ etc. corresponding to the wavelength $\lambda=C/\nu\,\mathrm{m}\mu$, where ν is a tabulation point, were determined applying the interpolation method.

As the interpolation method, the third-difference osculatory method was used. This method was first used by Judd[5] to interpolate the visibility function and thereafter by others[6] to interpolate the values of $E_\lambda\bar{x}_\lambda$ etc., given for every $10\,\mathrm{m}\mu$, in $1\,\mathrm{m}\mu$ intervals. In this method, the function in the interval between two successive values given in the table is expressed by such a third order curve that the tangent at one end of the curve is also the tangent to the curve in the adjoining interval.

Assume that the values of a function of λ, V_λ, are given in equal intervals of $10\,\mathrm{m}\mu$, and the first, second and third-order differences are as given in Table 1. Then, V_λ for $\lambda_0<\lambda<\lambda_0+10$ is given by

$$V_\lambda=V_{\lambda_0-10}+K_1\Delta_1V_{\lambda_0-10}+K_2\Delta_2V_{\lambda_0-10}+K_3\Delta_3V_{\lambda_0-10} \tag{8}$$

5) D. B. Judd: Bur. Stand. J. Res. **6** (1931) 465.
6) A. C. Hardy: *loc. cit.* p. 32.

where

$$\left.\begin{aligned} K_1&=(\lambda-\lambda_0+10)/10\\ K_2&=(\lambda-\lambda_0+10)(\lambda-\lambda_0)/200\\ K_3&=(\lambda-\lambda_0)(\lambda-\lambda_0-10)/2,000 \end{aligned}\right\}. \qquad (9)$$

Table 1.

$\lambda(\mathrm{m}\mu)$	V_λ	$\Delta_1 V_\lambda$	$\Delta_2 V_\lambda$	$\Delta_3 V_\lambda$
λ_0-10	V_{λ_0-10}			
		$\Delta_1 V_{\lambda_0-10}$		
λ_0	V_{λ_0}		$\Delta_2 V_{\lambda_0-10}$	
		$\Delta_1 V_{\lambda_0}$		$\Delta_3 V_{\lambda_0-10}$
λ_0+10	V_{λ_0+10}		$\Delta_2 V_{\lambda_0}$	
		$\Delta_1 V_{\lambda_0+10}$		
λ_0+20	V_{λ_0+20}			

Using this equation, the values of $E_\lambda\bar{x}_\lambda$ etc. for the desired ν are determind, but these are the values per unit width of the wavelength. The values $E_\nu\bar{x}_\nu$ etc. needed in the integration by ν, are obtained by converting them to the values per unit width of the wavenumber by multiplying $d\lambda/d\nu$. That is,

$$E_\nu\bar{x}_\nu=E_\lambda\bar{x}_\lambda\frac{d\lambda}{d\nu}=-\frac{C}{\nu^2}E_\lambda\bar{x}_\lambda\,. \qquad (10)$$

As mentioned above, the CIE data are given in every 10 mμ. It does not tell where the value becomes zero within the interval of 10 mμ. Therefore, it was assumed that the value becomes zero at a wavelength 10 mμ away from the wavelength at which the value is the nearest to zero. In the CIE data, the wavelength range in which any of the values $E_\lambda\bar{x}_\lambda$, $E_\lambda\bar{y}_\lambda$, $E_\lambda\bar{z}_\lambda$ does not become zero, is from 380 mμ to 770 mμ. Accordingly, by extending 10 mμ at both ends, one may assume that the values are given in the range from 370 mμ to 780 mμ. The wavenumbers corresponding to these limits are 27,027 cm^{-1} and 12,820 cm^{-1}. The range of wavenumber in which the values of $E_\nu\bar{x}_\nu$ etc. should be tabulated, was taken as from 13,000 cm^{-1} to 27,000 cm^{-1}. The interval in wavenumber was selected as 200 cm^{-1}, corresponding to 3 mμ in the short wavelength end and to 12 mμ in the long wavelength end so that the corresponding interval in wavelength should not exced 10 mμ except at the long wavelength end, where it is usually not of importance.

The conversion was performed using the relay computer. The results for the CIE A- and C-Illuminants are tabulated in Table 2. The values in the table are multiplied by a coefficient $\Delta\nu=200$ for convenience. If the values in the table are summed up, they give the tristimulus values X, Y, Z of the illuminant. If the value per unit width of wavenumber is needed, they must be divided by 200.

Directions for the use of tables are as follows. Let the r coefficient eflection

Table 2.

ν cm^{-1}	Illuminant A			Illuminant C		
	$E_A\bar{x}$	$E_A\bar{y}$	$E_A\bar{z}$	$E_C\bar{x}$	$E_C\bar{y}$	$E_C\bar{z}$
13000	2.5	0.1		1.2	0.1	
13200	5.0	2.4		1.3	1.2	
13400	9.2	3.6		2.9	1.4	
13600	20.9	8.2		5.8	2.5	
13800	43.1	14.4		13.5	4.4	
14000	84.5	30.0		28.9	10.0	
14200	156·7	56.5		58.9	20.9	
14400	287.4	103.5		117.1	42.1	
14600	542.9	196.6		239.9	87.0	
14800	946.9	344.9		446.6	162.5	
15000	1584.1	581.3		791.1	290.4	
15200	2548.4	946.0		1333.8	495.5	
15400	3765.6	1424.6		2045.6	773.2	
15600	5193.5	2019.2		2911.1	1131.8	
15800	6626.3	2682.7		3861.4	1563.1	
16000	8005.4	3420.8	1.1	4853.2	2073.6	0.8
16200	9021.4	4136.9	2.5	5688.4	2608.9	1.5
16400	9432.5	4748.8	3.0	6207.4	3124.9	1.5
16600	9293.0	5280.8	6.3	6425.8	3648.5	4.2
16800	8707.3	5705.0	7.8	6405.8	4199.2	5.9
17000	7819.0	6010.8	8.9	6177.7	4752.5	7.5
17200	6760.1	6191.4	11.7	5765.6	5281.2	10.3
17400	5677.4	6213.9	12.5	5213.3	5711.1	11.4
17600	4640.5	6100.3	14.6	4573.2	6011.6	14.3
17800	3700.4	5867.8	20.0	3884.1	6163.9	21.3
18000	2889.3	5541.5	30.3	3194.4	6124.8	33.7
18200	2200.7	5146.1	47.4	2534.1	5924.3	54.6
18400	1635.6	4709.4	74.1	1940.2	5583.9	87.7
18600	1170.3	4234.5	110.5	1424.2	5147.3	134.2
18800	792.4	3728.2	156.0	985.4	4634.8	193.3
19000	488.9	3200.4	207.1	626.7	4109.3	264.3
19200	257.7	2661.7	270.6	346.0	3575.8	362.2
19400	111.9	2120.7	374.9	158.7	3041.0	539.7
19600	31.8	1619.4	499.2	49.2	2532.5	780.0
19800	5.5	1216.2	618.9	10.6	2085.4	1063.9
20000	13.5	896.0	754.5	26.0	1700.5	1432.0
20200	36.4	668.9	913.8	76.9	1392.7	1910.7
20400	75.0	504.9	1106.9	169.5	1141.6	2503.7
20600	126.6	385.1	1357.2	307.3	937.7	3294.3
20800	186.9	299.6	1631.0	480.6	771.2	4202.4
21000	253.7	229.8	1914.3	692.5	627.1	5223.1
21200	321.3	177.1	2183.3	923.0	507.1	6269.9
21400	373.7	136.0	2358.1	1129.7	411.5	7122.9
21600	414.6	106.0	2460.9	1320.6	337.6	7833.0
21800	434.6	82.0	2464.6	1457.3	276.0	8261.7
22000	432.4	63.4	2361.2	1540.2	225.6	8403.1
22200	419.2	48.8	2216.7	1583.0	183.7	8368.8
22400	402.3	37.2	2076.4	1600.5	148.1	8261.9
22600	378.6	28.4	1918.5	1583.6	118.4	8020.1
22800	345.1	21.1	1723.2	1499.8	92.2	7487.0

ν cm^{-1}	Illuminant A			Illuminant C		
	$E_A\bar{x}$	$E_A\bar{y}$	$E_A\bar{z}$	$E_C\bar{x}$	$E_C\bar{y}$	$E_C\bar{z}$
23000	302.0	15.5	1491.2	1352.6	69.2	6677.5
23200	253.8	11.1	1241.6	1165.1	49.8	5699.9
23400	200.6	7.5	973.7	936.9	34.4	4550.6
23600	142.5	4.8	687.5	669.9	22.3	3237.9
23800	94.2	2.9	452.0	445.2	13.4	2139.8
24000	62.0	1.7	295.9	294.2	7.9	1406.9
24200	39.4	1.1	188.1	185.4	4.9	885.3
24400	23.2	0.7	111.1	107.4	2.9	512.4
24600	13.6	0.4	65.2	62.0	1.6	294.5
24800	9.1	0.4	44.2	41.3	1.0	196.4
25000	6.1	0.3	29.8	27.2	0.6	129.3
25200	3.6	0.2	17.6	15.5	0.3	73.3
25400	2.4	0.1	11.6	9.9	0.1	46.7
25600	1.7		7.8	6.5		30.6
25800	1.0		4.5	3.5		16.3
26000	0.6		3.0	2.1		10.2
26200	0.4		2.2	1.5		7.5
26400	0.2		1.4	0.9		4.3
26600	0.1		0.7	0.4		2.1
26800			0.3	0.2		0.9
27000						0.1
	109828.5	99999.6	35547.4	98041.3	100000.0	118100.4

for the light of wavenumber ν be R_ν, then the tristimulus values X, Y, Z of the reflected light are given by

$$\left.\begin{aligned} X &= \sum_{13,000}^{27,000} R_\nu E_\nu \bar{x}_\nu \Delta\nu/100,000 \\ Y &= \sum_{13,000}^{27,000} R_\nu E_\nu \bar{y}_\nu \Delta\nu/100,000 \\ Z &= \sum_{13,000}^{27,000} R_\nu E_\nu \bar{z}_\nu \Delta\nu/100,000 \end{aligned}\right\} \tag{11}$$

The problem under consideration is to determine the interference color of a stained lens surface coated with anti-reflection film. The program for computation was planned to calculate the tristimulus values of reflected light for various optical thicknesses of the "stain", n_1d_1, the optical thickness of the anti-reflection coating, n_2d_2 being given.

To do this, at first, $\sin\delta_2$ and $\cos\delta_2$ for the uppermost layar were calculated at every calculation point and their values were memorized by the machine and used in common in the calculation for every value of n_1d_1.

Following the method outlined above, the calculation was performed using FACOM-128 automatic relay computer. FACOM-128 is a digital computer of

floating system, built for universal purpose. The number of effective figures is eight. The time needed for the calculation in converting the table of $E_\lambda\bar{x}_\lambda$ into the table of $E_\nu\bar{x}_\nu$ in equal intervals of ν, was 14 min, amounting to 42 min in total for $E_\nu\bar{x}_\nu$, $E_\nu\bar{y}_\nu$, $E_\nu\bar{z}_\nu$. To prepare from them an input tape necessary for the next step, it took 4 min. Colorimetric calculation for a given n_1d_1 took 90 min for 7 values of n_2d_2.

The results of computation will be published in a separate paper[7].

4. Conclusion

As it is necessary for colorimetric calculation to take many calculation points, it is too laborious to do it by hands, whereas with an automatic computer, repeated calculations are very easily performed.

It is not suited to a mechanical computer of slow speed to calculate separately the values of trigonometrical functions required in the determination of interference color. Hence the program was designed so as to calculate values of the functions by means of the sum-rule of trigonometrical functions.

It was found that the numerical integration using equal intervals in wave-number is preferable to the integration using equal intervals in wavelength. It also gives a possibility of saving the labor in referring to the trigonometrical tables because numerical values in function tables are generally given at equal intervals of variables.

If it is possible to make use of an electronic computer of large capacity for memory, the device described in this paper will become unnecessary and the calculation inclusive of the change of refractive index with the wavelength will be performed easily.

The author wishes to express his thanks to members of the Calculation Center of the Fuji Automatic Computer, who helped him in performing calculations involved in this work.

7) K. Miyake: Science of Light **6** (1957) 85.

Detection of Stains Formed on Lens Surface

Kazuo MIYAKE

Institute for Optical Research, Tokyo University of Education
Shinjuku-ku, Tokyo

(Received November 15, 1957)

Abstract

When detection is made by using reflection of light, detectable minimum of optical thickness of stains formed on lens surface is determined to be 13–20 mμ.

As the angle of incidence of the light increases, the accuracy falls.

The interference color of stained lens surfaces coated with anti-reflection film is determined using an automatic relay computer.

The results are plotted on the CIE chromaticity diagram and the color difference is calculated.

The higher the refractive index of substrate glass, the smaller the detectable minimum of stain thickness when coated with anti-reflection film.

Amber coating has an effect similar to using a glass of low refractive index and may have a possibility to prevent the appearance of irregularity in the interference color of anti-reflection coatings.

1. Introduction

In the course of lens making, an anomalous layer called "stain" appears at times on lens surfaces.

To prevent the reflection of light at lens surfaces, nearly all lenses of high grade are now coated with anti-reflection films. If the reflection-reducing coating is deposited by evaporation on the lens surface on which a stain has been formed, the stain is easily detected as irregularity in the color of the coating.

In optical workshops, they examine lens surfaces generally with reflected light and reject the lens on the surface of which any stain is detected. But slight stains which are unnoticed in early stages, become clearly visible after the coating was made which is very annoying to lens makers.

By analysing the above phenomenon, tolerable stain thickness for avoiding the otherwise cumbersome procedure was determined.

2. The Method of Detection Using Reflected Light

Ordinary method of detecting stains, adopted nowadays in optical workshops, is to let a light from a wide source such as the blue sky or a frosted shade of incandescent electric lamp reflect at lens surfaces and to examine the surface. In

this method, detection is by the difference in reflectivity between the parts stained and unstained.

Although the accuracy of detection obtained by this method has already been calculated by Doi[1], a similar calculation is repeated to make a comparison with the results obtained in the following sections and to enable a more detailed discussion.

Assume that the stain has a structure shown in Fig. 1.

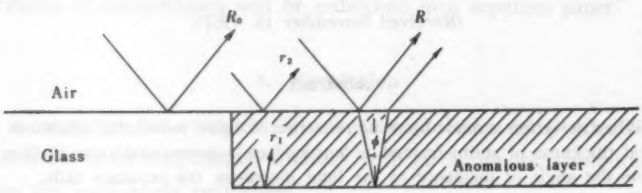

Fig. 1. Structure of the stain

The case of normal incidence of light is considered at first. Let r_1, r_2 be the amplitude reflection coefficients at the interfaces stain—glass and air—stain, n_0, n the refractive indices of glass and stain, R_0, R the amplitude reflection coefficients of glass surface and stained surface. Then,

$$r_1=\frac{n-n_0}{n+n_0} \qquad r_2=\frac{1-n}{1+n} \tag{1}$$

$$R=\frac{r_1+r_2e^{i\Delta}}{1+r_1r_2e^{i\Delta}} \qquad R_0=\frac{r_1+r_2}{1+r_1r_2} \tag{2}$$

where $\Delta=(4\pi/\lambda)nd$, and d and λ being the thickness of stain and the wavelength of light considered. Taking the contrast of lights reflecting at the glass surface and at the stained surface as

$$V=\frac{|R_0|^2-|R|^2}{|R_0|^2+|R|^2}, \tag{3}$$

after some calculations, it is given as

$$V=\frac{4r_1r_2(1-r_1^2)(1-r_2^2)\sin^2\Delta/2}{2(r_1+r_2)^2(1+r_1r_2)^2-4r_1r_2\{(r_1+r_2)^2+(1+r_1r_2)^2\}\sin^2\Delta/2}. \tag{4}$$

Expressing the least contrast perceptible to the naked eye as V_{min}, the minimum detectable phase difference angle Δ is given by

$$\sin^2\frac{\Delta}{2}=\frac{(r_1+r_2)^2}{2r_1r_2}\,\frac{(1+r_1r_2)^2V_{min}}{(1-r_1^2)(1-r_2^2)+\{(r_1+r_2)^2+(1+r_1r_2)^2\}V_{min}} \tag{5}$$

Assuming r_1, r_2, V_{min} to be small compared with unity and taking $r_1\fallingdotseq r_2$, we obtain as an approximate expression,

1) Y. Doi: Tech. Rep. Japan Camera Res. Ass. No. 1 (Nov. 20, 1956) p. 3 (in Japanese).

$$\sin^2\frac{\overline{\Delta}}{2}=2V_{min} \qquad (6)$$

The value of V_{min} depends on the conditions of observation. The value known as the Fechner fraction in photometry, was adopted here. When the average intensity I is sufficiently high, the minimum perceptible difference in intensity ΔI is given as $\Delta I/I=1/60$. As $\Delta I/I$ is equal to $2V_{min}$, taking $V_{min}=1/120$, the refractive index of stain $n=1.47$ and the refractive index of the glass $n_g=1.74$, 1.63, 1.52, the detectable minimum of optical thickness $\overline{nd}$ of the stain was calculated and shown in Table 1. The wavelength of light is taken as the one having the maximum visual sensitivity, that is, $\lambda=555\,\mathrm{m}\mu$.

Table 1.

n_g	1.74	1.63	1.52	According to (6)
$\overline{nd}$	13.0	14.1	21.1	$11.5\,\mathrm{m}\mu$

From this result, it is concluded that the detectable minimum value $\overline{nd}$ of stain on glass used for optical purpose is about from 13 to 20 $\mathrm{m}\mu$ and the higher the refractive index of the glass, the smaller becomes this minimum.

3. Effect of Incident Angle

The expressions (1) and (2) are given for the case of normal incidence. In the case of oblique incidence, using the Fresnel coefficients for p- and s-components of light as the amplitude reflection coefficients in corresponding cases, the expressions (2) and (4) remain unchanged for each of the two components except that $\Delta=(4\pi/\lambda)nd\cos\phi$, ϕ being the angle of refraction in the stain.

As the result, the form of the expression (5) remains the same and using the approximate expression (6) for $r_1=r_2$, the accuracy of detecting $\overline{\Delta}$ does not change in the first approximation. Therefore $\overline{nd}$ becomes larger in proportion to the factor $\sec\phi$.

To verify this conclusion, an observation was made using the apparatus constructed previously for detecting stains[2]. A disc of SK5 glass was mounted on a supporter S, shown in Fig. 2. A half of the surface of the specimen was covered with paraffin and the exposed half was etched by dipping it in a 1N HNO_3 aqueous solution at 30°C for 25 seconds.

The glass surface was observed using a light reflected at it. The angle of incidence was changed by the rotation of S accompanied with the corresponding

2) K. Miyake: Science of Light, (Tokyo) **5** (1956) 130.

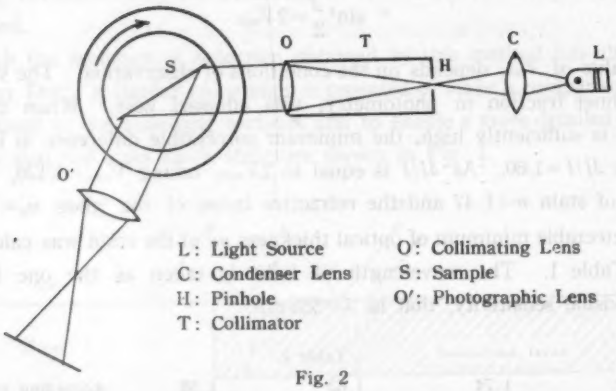
O
T
C
L
S
H
O'
L: Light Source
C: Condenser Lens
H: Pinhole
T: Collimator
O: Collimating Lens
S: Sample
O': Photographic Lens

Fig. 2

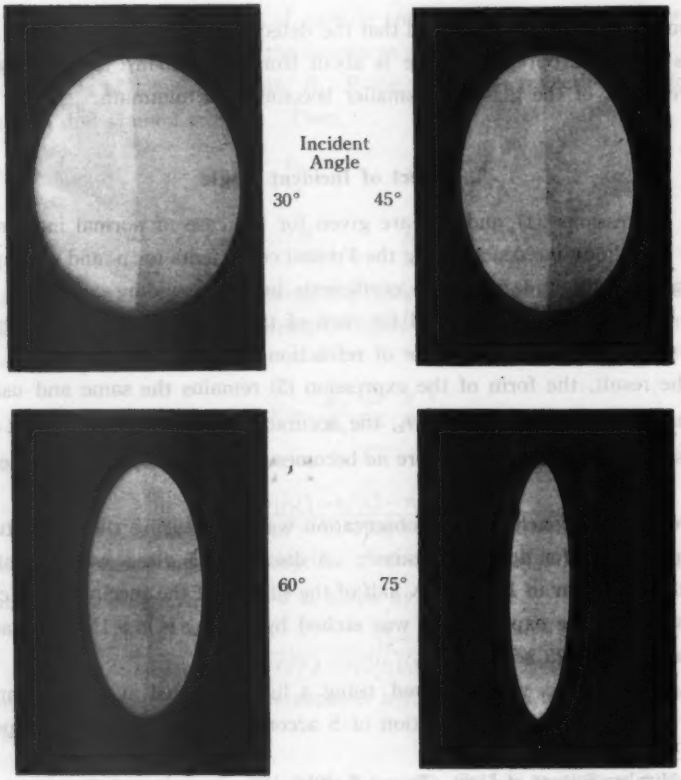
Incident Angle
30°
45°
60°
75°

Fig. 3

change of the direction of sight. The result is shown in Fig. 3. The contrast becomes lower with the increasing incident angle.

A conclusion obtained from this result is that the smaller the angle of incidence, the smaller the detectable stain thickness provided that the light used is sufficiently strong in intensity and that no disturbing factor such as reflection at back surface inconveniences the observation.

4. Irregularity of Color of Anti-reflection Films

The interference color of thin films has been investigated by Kubota[3] and Mönch[4]. Kubota determined the chromaticity of color of films deposited on glass surface to various thickness, using the colorimetric method adopted by the CIE committee on colorimetry.

If the stain is so slight that, after being coated with anti-reflection film, there is no perceptible difference between the interference color on the stain and that on the rest of the surface, such stains can be left out of the question in practice. The maximum optical thickness of permissible stain should then be determined, for which purpose the interference color was examined for stains of known thicknesses.

The required calculation was performed on an automatic relay computer. To facilitate the operation, the colorimetric calculation was carried out using the wavenumber as the variable, not the wavelength as usually adopted. Details of the computation will be published in a separate paper[5].

The structure of the stain coated with anti-reflection film was assumed to be a double layer shown in Fig. 4, the refractive index n_0 of the substrate glass being 1.74, 1.63, and 1.52, the refractive indices of the stain and the reflection-reducing film, n_1, n_2 1.47 and 1.38 respectively.

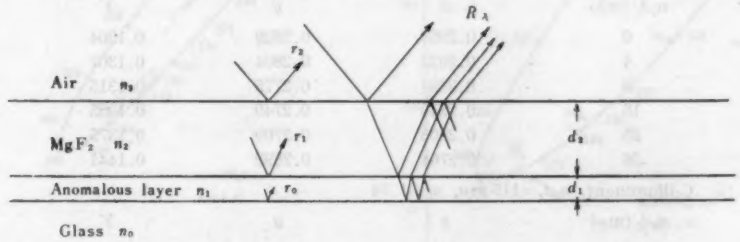

Fig. 4

3) H. Kubota: J. Opt. Soc. Am. **40** (1950) 146.
4) Mönch: Optik **9** (1952) 97.
5) K. Miyake: Science of Light, (Tokyo) **6** (1957) 77.

As the light source, the C-illuminant of CIE was used except in one case, in which the A-illuminant of CIE was used.

Table 2.

(1) A-illuminant, $n_2d_2=138.9\,\mathrm{m}\mu$, $n_0=1.74$

n_1d_1 (mμ)	x	y	Y
0	0.3934	0.2757	0.03059
1	0.3832	0.2723	0.03028
2	0.3732	0.2693	0.03008
4	0.3538	0.2643	0.02999
9	0.3120	0.2588	0.03156
16	0.2747	0.2652	0.03806
25	0.2597	0.2865	0.05343
36	0.2694	0.3159	0.08187

(2) C-illuminant, $n_2d_2=138.9\,\mathrm{m}\mu$, $n_0=1.74$

n_1d_1 (mμ)	x	y	Y
0	0.2317	0.1432	0.03118
1	0.2263	0.1401	0.03138
4	0.2124	0.1336	0.03265
9	0.1960	0.1297	0.03690
16	0.1844	0.1342	0.04722
25	0.1814	0.1486	0.06744
36	0.1871	0.1707	0.10137

(3) C-illuminant, $n_2d_2=138.9\,\mathrm{m}\mu$, $n_0=1.63$

n_1d_1 (mμ)	x	y	Y
0	0.2696	0.2268	0.06796
4	0.2585	0.2179	0.06886
9	0.2469	0.2098	0.07144
16	0.2348	0.2036	0.07772
25	0.2258	0.2026	0.09003
36	0.2224	0.2088	0.11072

(4) C-illuminant, $n_2d_2=138.9\,\mathrm{m}\mu$, $n_0=1.52$

n_1d_1 (mμ)	x	y	Y
0	0.2950	0.2829	0.1304
4	0.2923	0.2804	0.1307
9	0.2891	0.2775	0.1315
16	0.2849	0.2740	0.1335
25	0.2803	0.2709	0.1375
36	0.2764	0.2692	0.1441

(5) C-illuminant, $n_2d_2=115\,\mathrm{m}\mu$, $n_0=1.74$

n_1d_1 (mμ)	x	y	Y
0	0.4601	0.3924	0.07953
4	0.4499	0.3698	0.06825
9	0.4242	0.3305	0.05634
16	0.3674	0.2640	0.04403
25	0.2868	0.1912	0.03612
36	0.2221	0.1532	0.03887

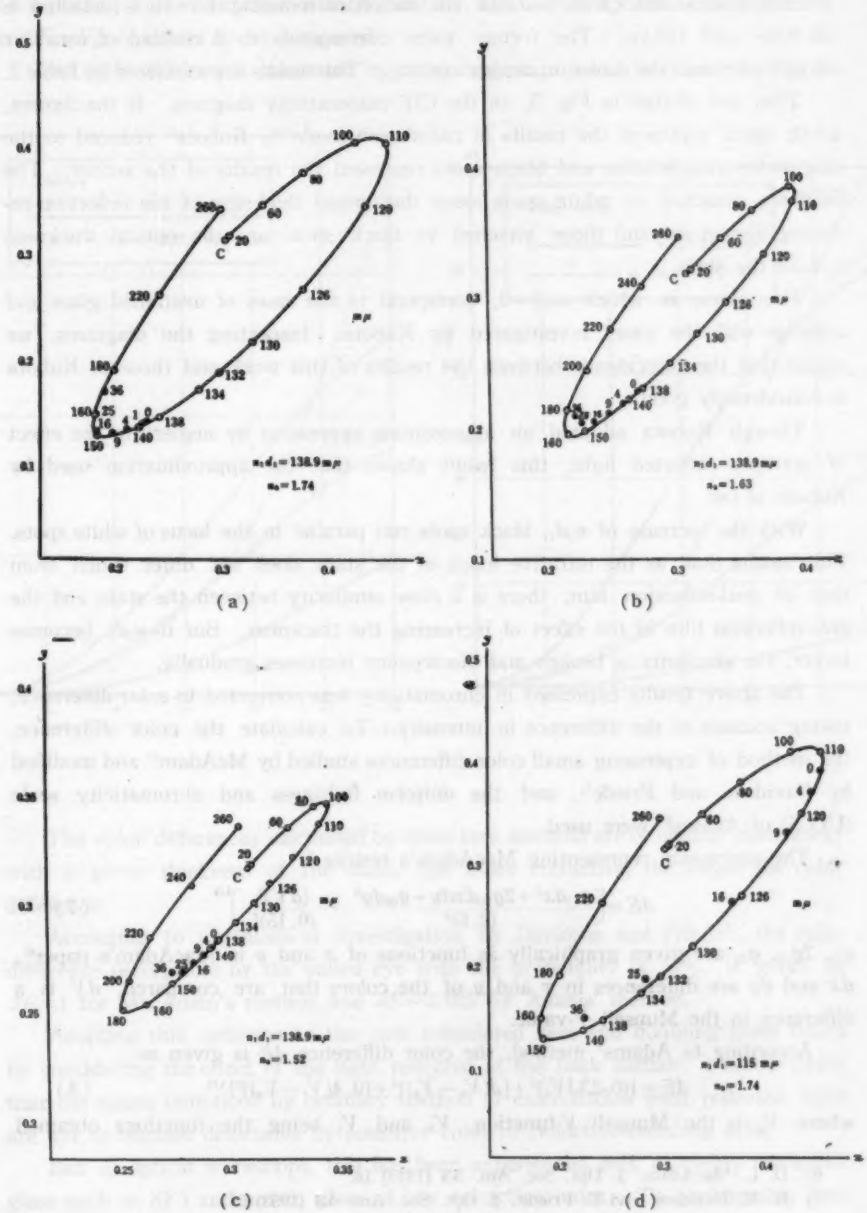

Fig. 5

The optical thickness, n_2d_2 of the reflection-reducing film was selected as 138.9 mμ and 115 mμ. The former value corresponds to a coating of sensitive purple color and the latter to amber coating. The results are tabulated in Table 2.

They are plotted in Fig. 5, on the CIE chromaticity diagram. In the figures, white spots represent the results of calculation made by Kubota[5] reduced to the case under consideration and black spots represent the results of the author. The numbers attached to white spots mean the optical thickness of the reflection-reducing film in mμ and those attached to black spots are the optical thickness n_1d_1 of the stain.

The cases, in which $n_1d_1=0$, corrspond to the cases of unstained glass and coincide with the cases investigated by Kubota. Inspecting the diagrams, we notice that the coincidence between the results of this work and those of Kubota is considerably good.

Though Kubota adopted an approximate expression by neglecting the effect of multiply reflected light, this result shows that the approximation used by Kubota is fair.

With the increase of n_1d_1, black spots run parallel to the locus of white spots. This means that, as the refrative index of the stain does not differ much from that of anti-reflection film, there is a close similarity between the stain and the anti-reflection film in the effect of increasing the thickness. But if n_1d_1 becomes larger, the similarity is broken and discrepancy increases gradually.

The above results expressed in chromaticity was converted to color difference, taking account of the difference in intensity. To calculate the color difference, the method of expressing small color differences studied by McAdam[6] and modified by Davidson and Friede[7], and the uniform lightness and chromaticity scale (ULCS) of Adams[8] were used.

The expression representing MacAdam's results is

$$\Delta E=\left[\frac{g_{11}dx^2+2g_{12}dxdy+g_{22}dy^2}{(2.5)^2}+\frac{(dV)^2}{(0.15)^2}\right]^{1/2} \qquad (7)$$

g_{11}, $2g_{12}$, g_{22} are given graphically as functions of x and y in MacAdam's paper[6], dx and dy are differences in x and y of the colors that are compared, dV is a difference in the Munsell V-value.

According to Adams' method, the color difference ΔE is given as

$$\Delta E=\{(0.23\Delta V_y)^2+[\Delta(V_x-V_y)]^2+[0.4(V_z-V_y)]^2\}^{1/2} \qquad (8)$$

where V_y is the Munsell V-function, V_x and V_z being the functions obtained

6) D. L. MacAdam: J. Opt. Soc. Am. **33** (1943) 18.
7) H. R. Davidson and E. Friede: J. Opt. Soc. Am. **43** (1953) 581.
8) E. Q. Adams: J. Opt. Soc. Am. (1942) 168.

by replacing Y in V-function with X_c and Z_c, and $\Delta(V_x - V_y)$ means a difference in $(V_x - V_y)$ of colors to be compared.

The color differences calculated by using these expressions are shown in Fig. 6.

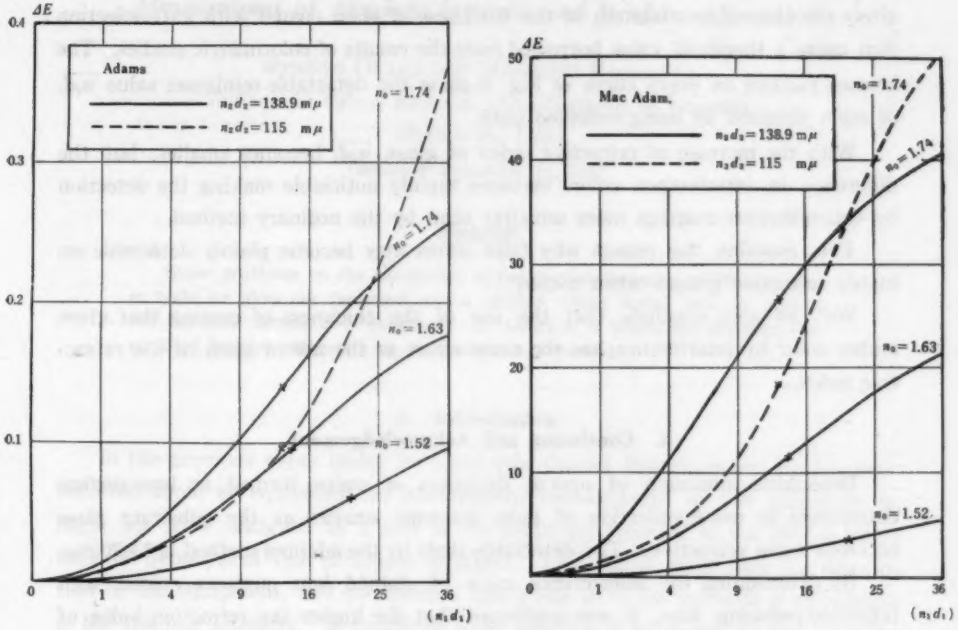

Fig. 6

The color differences calculated by these two methods are of similar tendencies: with a given thickness of the stain, the more refractive, the larger the color difference.

According to a statistical investigation by Davidson and Friede[7], the color difference perceptible by the naked eye with the probability of 50%, is given as $\Delta E = 1$ for MacAdam's method and $\Delta E = 0.025$ for Adams' method.

Adopting this criterion to the case considered here and doubling these limits by considering the effect of the light reflected at the back surface, it seems likely that the stains unnoticed by ordinary method of examination with reflected light are apt to become detectable by sensitive color of reflection-reducing films.

But in optical workshops, this has been experienced only in highly refractive glass such as SF3 and not in glass of low refractive index. To explain this fact satisfactorily, the perceptible limit of the color differenec must be chosen approx-

imately as $\Delta E=20$ for MacAdam's method and $\Delta E=0.1$ for Adams' method. But it may be too arbitrary to do so. The values of the perceptible limit cited above were determined under a special condition and, strictly speaking, they are not applicable to all cases. So we must give up the attempt to determine quantitatively the detectable minimum of the thickness of stain coated with anti-reflection film using a threshold value borrowed from the results of colorimetric studies. The crosses marked on every curve in Fig. 6 show the detectable minimum value $\overline{n_1 d_1}$ of stain obtained by using reflected light.

With the increase of refractive index of glass, $\overline{n_1 d_1}$ becomes smaller, but the difference in interference colors becomes rapidly noticiable making the detection by anti-reflection coatings more sensitive than by the ordinary method.

This explains the reason why faint stains may become plainly detectable on highly refractive glasses when coated.

We can also conclude that the use of the thickness of coating that gives amber color by interference has the same effect as the use of glass of low refractive index.

5. Conclusion and Acknowledgement

Detectable minimum of optical thickness of stains formed on lens surface determined by using reflection of light becomes smaller as the substrate glass becomes more refractive. The detectable limit by the adopted method is 13–20 mμ.

By determining the interference color of stained lens surfaces coated with reflection-reducing film, it was confirmed that the higher the refractive index of the glass, the more rapidly grows the irregularity of the interference color.

The amber coating has the same effect as using the glass of low refractive index and may be effective in preventing the appearance of irregularity in the color of coatings.

This work has been made as a part of research projects concerning "Measurement of the performance of photographic lenses and improvement of their productivity" of Japan Camera Research Association.

Research expenses were party borne by the Ministry of International Trade and Industry. A part of computation performed on the computer was serviced freely by the Calculating Center of Fuji Automatic Relay Computer.

The author wishes to express his thanks to these two organizations.

Photoelectric Studies of Near Infrared OH Emissions of Night Sky (II)
Measurement of Absolute Intensity and Brightness Standard

Ryumyo ONAKA and Masatoshi NAKAMURA
Institute for Optical Research, Tokyo University of Education
Shinjuku-ku, Tokyo

(Received December 14, 1957)

Abstract

Some problems on the estimation of the absolute intensity of OH emissions in night air glow are discussed, and a method which seems best to express the absolute intensity is proposed. In addition, a brightness standard constructed for the calibration of photometer is described.

1. Introduction

In the previous paper under the same title, Ogawa, Nakamura and Hashizume[1] reported about an equipment for photoelectric measurement of OH emissions in night air glow assigned as a part of the night sky research in the 1957–8 International Geophysical Year programs in Japan. That report gives only the description of the equipment, and no mention was made as to the methods of calculation of the absolute intensity. It would be most practical if all report on the intensity measurement of the air glow are made in absolute units. The estimation of the the absolute intensity of OH emissions involves, however, more cumbersome problems than that of atomic lines in the air glow.

In this paper a method of estimation of the absolute intensity of OH bands will be discussed, and a brightness standard which is in use in the observatories at Shodoshima (Institute for Optical Research) and Maruyama (Tokyo Astronomical Observatory) will be described.

2. Characteristic Problems in the Estimation of Absolute Intensity of OH Emissions

Some cumbersome problems are inevitable in the estimation of the absolute intensity of OH emissions because of the following reasons:

1° The spectrum of OH emission in air glow is not of single lines, but has

1) M. Ogawa, M. Nakamura and A. Hashizume: Science of Light **5** (1956) 139.

a band structure composed of a great number of lines extending over a wide wavelength range from the visible to the infrared.

2° The main part of OH emissions falls in the near infrared region, where photoelectric sensitivity of photo tubes is so low that individual lines in the bands can not be measured by ordinary photoelectric devices. Merely the total intensity of a band or several bands is measurable.

3° The relative intensities of the bands have not yet been established. Theoretical values calculated under some assumptions[2)3)] have been reported. These values are most reliable at present[4)], but some experimental results are contradictory[5)].

4° Studies of extinction, scattering and absorption in air are not yet sufficient in the near infrared region to give accurate corrections to the observed intensity of the night sky emissions.

5° The two color photometer[6)] which is proved to be effective for OI λ 5577 line in eliminating the extra-terrestrial components (mainly light from stars and the zodiacal light) is not available for OH emissions.

The intensity of band emissions would be completely defined if the intensities of all individual lines are given. If, however, the the relative intensity of individual lines is known in a band or in a band system, an expression of the total intensity of a band or of a band system would be sufficient to define the intensity.

The relative intensity of lines in a single band corresponding to a vibrational transition is possibly defined by means of the rotational temperature and the relative intensity of the multiplet components. The rotational temperature of OH bands in night air glow was measured by several authors[7)]. Meinel [7] gave 265°K as the rotational temperature and 0.317 as the intensity ratio of $^2\Pi_{1/2}$ and $^2\Pi_{3/2}$ from his observations at a moderate latitude.

The deflections of photometer are due not only to the air glow emissions but also to the light from stars and to the zodiacal light. These extra-terrestrial

---

2) H. S. Heaps and G. Herzberg: Zeits. f. Phys. **133** (1952) 48.
3) F. E. Roach: *The International Geophysical Year Instruction Manual IV*, Pergamon Press, London (1956), p. 76.
4) A. V. Jones: Nature **172** (1953) 496.
H. P. Gush and A. V. Jones: J. Atm. Terr. Phys. **7** (1955) 285.
5) N. I. Eedorova: Astronomchski, Zhurnal, **34** (1957) 1247.
6) F. E. Roach and H. B. Pettit: J. Geophys. Res. **56** (1951) 325.
M. Huruhata, T. Nakamura and H. Tanabe, Tokyo Astronomical Bulletin, Sec. Ser. **94** (1957) 1005.
7) A. B. Meinel: Astrophys. J. **112** (1950) 120.
J. Cabannes, J. Dufay: Compt. Rend. **232** (1951) 426.
C. Oliver: Phys. Rev. **90** (1953) 1118.

components must be substracted from the original values of deflections of the photometer. If an assumption that the spectra of the star light and of the zodiacal light are both G_0 type in average is allowed, one can estimate the intensity of the extra-terrestrial components at a wavelength in the infrared region from those at 5300 A, at which the intensities are easily measured because of the absence of contribution of the air glow. The variation of the extra-terrestrial components with the zenith distance is known to be small at 5300 A which would also be the case with the infrared region. The effect of absorption by water vapor in the extra-terrestrial components calculated from the amount of precipitable water and the absorption coefficients of water vapor is only 6% in summer and 3% in winter for our photometer. As the actual contribution of the extra-terrestrial components in photometer deflection in the near infrared region is only about 20%, somewhat rough estimation of this background would be tolerable.

From above reasons, it would be possible to give the proper deduction of the extra-terrestrial components from the deflections of the photometer.

The effects of extinction, scattering and absorption by the earth's atmosphere for the air glow components can be eliminated by means of "the mean value method" in which the multiplication factors for observed values differing in zenith distance are found from their mean values. This is based on the reasoning that the mean of air glow intensities observed at one place is the same at any other place, provided that observations are made for a long period.

3. Calculation of the Absolute Intensity of OH Emissions

The deflection of the photometer will be given by the following formula.

$$D=A\int_{\lambda} S(\lambda)T(\lambda)B(\lambda)d\lambda=A\int_{\lambda} G(\lambda)B(\lambda)d\lambda\,,$$

where D: deflection of the photometer,
A: sensitivity of electronic accessory of the photometer,
$S(\lambda)$: spectral sensitivity of the photo tube used,
$T(\lambda)$: overall spectral transmission of the optical elements,
$G(\lambda)=S(\lambda)\cdot T(\lambda)$,
$B(\lambda)$: brightness of the night sky,
λ: wavelength.

$B(\lambda)$ can be divided into two components, namely the air glow emissions and the extra-terrestrial lights.

$$B(\lambda)=B_{\text{a.g.}}(\lambda)+B_{\text{e.t.}}(\lambda)$$

As the air glow emissions consist of a number of lines,

$$D=A\sum_{\lambda}G(\lambda)\tilde{B}_{a.g.}(\lambda)+A\int_{\lambda}G(\lambda)B_{e.t.}(\lambda)d\lambda\,,$$
$$=D_{a.g.}+D_{e.t.}\,,$$

where $\tilde{B}_{a.g.}(\lambda)$ means the integrated brightness over a spectral line or a narrow spectral band. Both $S(\lambda)$ and $T(\lambda)$ and therefore $G(\lambda)$ can be determined from laboratory measurements. $B_{e.t.}(\lambda)$ can be calculated from photometric data at 5300 A and the spectral distribution of the extra-terrestrial coponents. A can be determind by using a brightness standard of known spectral distribution and absolute intensity. If the standard emits only a monochromatic or a nearly monochromatic radiation of wavelenght λ_0, the deflection of the photometer for this standard is

$$D_0=AG(\lambda=\lambda_0)B_0\,,$$

or

$$A=D_0/G(\lambda=\lambda_0)B_0\,,$$

where B_0 is the known brightness of the standard. The extra-terrestrial part in the photometer deflections is, therefore,

$$D_{e.t.}=\frac{D_0}{G(\lambda=\lambda_0)B_0}\int_{\lambda}G(\lambda)B_{e.t.}(\lambda)d\lambda_0\,.$$

As the relative intensities of spectral lines or bands in air glow would not vary with time or place, we can put

$$\tilde{B}_{a.g.}(\lambda)=E\cdot\tilde{F}(\lambda)\,,$$

where E: a constant,

$\tilde{F}(\lambda)$: relative intensity of the spectral components (lines or bands) in the air glow.

Then,

$$D_{a.g.}=D-D_{e.t.}=\frac{D_0E}{G(\lambda=\lambda_0)B_0}\Sigma G(\lambda)\tilde{F}(\lambda)\,,$$

or

$$\tilde{B}_{a.g.}(\lambda)=\frac{D-D_{e.t.}}{D_0}B_0\frac{G(\lambda=\lambda_0)\tilde{F}(\lambda)}{\sum_{\lambda}G(\lambda)\tilde{F}(\lambda)}\,.$$

At present, relative intensities $\tilde{F}(\lambda)$ of OH bands are not known for certain. It seems best to express the absolute intensity of OH emission in the air glow provisionally by $(D-D_{e.t.})B_0/D_0$ and $G(\lambda)$, since $\tilde{B}_{a.g.}(\lambda)$ values can be easily calculated from the above equation after the exact $\tilde{F}(\lambda)$ values are found.

4. Brightness Standard

A brightness standard was constructed to determine the absolute sensitivity

of the photometer. This standard, which is shown in Fig. 1, can be easily mounted on the air glow photometer by means of a shoe. The light source of the standard is a midget tungsten lamp which is lighted at a current of 110 ma dc, while its normal rate is 300 ma. The lamp illuminates a disk of opal glass which is placed 40 cm apart from the lamp. An interference filter of maximum transmission at 8900 A was inserted between the lamp and the glass disk. The half width of the spectral transmission of the filter is 300 A. The opal glass disk is 12 cm in diameter and is large enough to cover the entire field of view of the photometer.

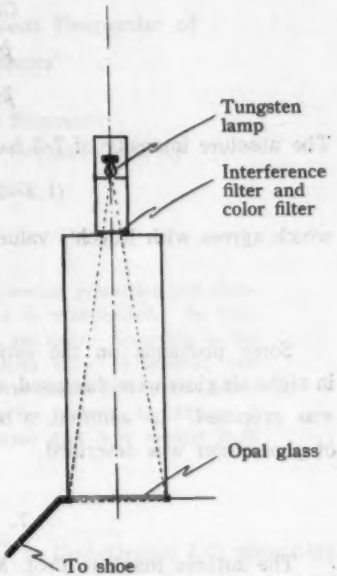

Fig. 1.

The brightness of the opal glass was calibrated by means of a thermocouple and a Mazuda radiation standard lamp. The brightness of the standard by 110 ma current is 2.61×10^{-3} microwatts/cm^2 steradian, which corresponds to 1.17×10^{10} quanta/sec cm^2 steradian for photons of 8900 A, or to 1.47×10^{5} rayleighs for the air glow intensity.

5. Absolute Intensity of OH Emissions in the Air Glow

The intensity of OH emissions in the air glow greatly varies with time and direction viewed. The deflection of the photometer is from about one tenth to a quarter of that for the standard, when it is directed to zenith in ordinary clear nights. The extra-terrestrial components are estimated to be about one thirtieth of the brightness standard, so the deflection due to the air glow alone is from one fifteenth to one fifth of that of the standard.
Then

$$\frac{D}{D_0}=\frac{1}{15}\sim\frac{1}{5},$$

$$B_0=1.47\times10^{5} \text{ rayleighs at 8900 A,}$$

$$DB_0/D_0=(1.0\sim3.0)\times10^{4} \text{ rayleighs.}$$

If the relative intensities of OH bands given by Roach in the IGY instruction manual[3] are used,

$$G(\lambda=8900\,\text{A})=5.0\,,$$

$$\tilde{F}(7\text{-}3\ \text{band})=47\,,$$

$$\tilde{F}(\lambda)G(\lambda)=1998\,.$$

The absolute intensity of 7-3 band of OH emissions of the air glow is, therefore,

$$(1.2\sim3.6)\times10^3\ \text{rayleighs},$$

which agrees with Roach's value of 1940 rayleighs[3].

6. Summary

Some problems on the estimation of the absolute intensity of OH emissions in night air glow were discussed, and a method of expressing the absolute intensity was proposed. In addition, a brightness standard constructed for the calibration of photometer was described.

7. Acknowledgement

The authors thank to Prof. M. Huruhata and Mr. T. Nakamura of the Tokyo Astronomical Observatory for their instructive discussions.

Influence of Flux on the Luminescent Properties of Cu-activated CaS Phosphors*

Sumitada ASANO and Takashi KISHIMOTO

Department of Physics, Faculty of Science, Okayama University

(Received December 5, 1957)

Abstract

The influence of addition of flux on the luminescent properties and ultraviolet absorption of Cu-activated CaS phosphors is investigated. As flux, sulfates, fluoride and chlorides of Li, Na and K are used. According to the results of experiments, Cu-activated CaS phosphors show, in general, two emission bands at about 430 mμ and 495 mμ and the sulfate and fluoride fluxes intensify the latter band, whereas chloride fluxes the former. In addition, it may be inferred that the latter band originates from CaS host crystal itself and the former from Cu-activator located in it.

1. Introduction

The effect of the flux such as NaCl and KCl in Cu-activated ZnS phosphors has been, to some extent, clarified by several investigators[1)-4)]. According to the recent investigations the pair of Cu-ion and Cl-ion, which are located substitutionally in CdS host crystals plays the essential role also for the photoconductivity of CdS crystals[5)]. On the other hand, for CaS phosphors sulfates and fluorides of alkali-metals such as Na_2SO_4, LiF, NaF etc. have been used customarily as flux[6)]. However, effect of these fluxes on the Cu-activated CaS phosphors has not been completely clarified. This paper deals with the influence of flux added to Cu-activated CaS phosphors on their visible luminescence and ultraviolet absorption.

2. Structure and Composition of host crystal.

The phosphors submitted to the experiments were prepared by Lenard's method, i.e. they are synthesized by heating the mixture of pure sulfur and CaO powder at 950°C for 20 min. in an electric furnace after the addition of adequate quantities of flux and activator. As the activator $CuSO_4$ and as the flux sulfate,

* The results presented in this paper were briefly reported at the Autumn Meeting, held at Okayama in October 1957, of the Society of Applied Physics (Japan).

1) F. A. Kröger and J. E. Hellingman: J. Electrochem. Soc. **93** (1948) 156, **95** (1949) 68.
2) R. H. Bube: J. Chem. Phys. **19** (1951) 985.
3) R. H. Bube: J. Chem. Phys. **20** (1952) 708.
4) F. A. Kröger et al: Physica **15** (1949) 990.
5) R. H. Bube and S. M. Thomsen: J. Chem. Phys. **23** (1954) 15, 18.
6) F. Schmidt: Ann. d. Phys. **19** (1932) 211.

chloride or fluoride of Li, Na or K were used. Proportions of activator and flux added are shown in weight percent.

Sulfur was purified by thrice-repeated sublimation and purified CaO powder was prepared from $CaCO_3$[7,8]. In heating the mixture, double crucible was used to avoid the oxidation.

According to the current view, in Lenard's method, host crystals are composed during the heating by following reaction[9].

$$4S+4CaO \longrightarrow 3CaS+CaSO_4 \quad (2.1)$$

In this method fairly large quantity of $CaSO_4$ is inevitably contained in the host crystals in addition to CaS. X-ray inspection by powder method showed that the host crystals are the mixture of regular CaS and $CaSO_4$ crystals, regardless of the sort and quantity of added flux. Further, any trace of CaO crystal was not recognized with the sample prepared under the above mentioned conditions. In order to determine the ratio of the amount of $CaSO_4$ to the total quantity of the host crystals, the amount of sulfate radicals in the prepared phosphors was measured by chemical analysis. 5 g of the phosphor is suspended in 20 cc of hot acetic acid (conc. acetic acid 1: water 4). In this procedure CaS crystals in the mixed crystal are decomposed by forming H_2S gas, whereas most part of $CaSO_4$ crystals remain suspended in liquid. This turbid liquid is introduced into 500 cc of boiling water. After stirring for a long time, the $CaSO_4$ crystals may be dissolved gradually and clear liquid is obtained.

The amount of sulfate radicals in the clear liquid may be determined by making the sulfate radicals precipitate as $BaSO_4$[10].

The results obtained are shown in Table I. In Table I the quantity of sulfate radicals, which originate from activator and flux (when sulfate of alkali-metal is used as flux) are subtracted from the results of analysis. Referring to the same table, we can point out that the proportion of sulphate radical in the host crystals is in good agreement with the value 26.5% expected from the reaction (2.1), regardless of the sort and quantity of the flux used.

From the results stated above, we can infer that the optical properties of pure CaS phosphor may be known, if from the optical properties of CaS phosphor pre-

---

7) P. Lenard and V. Klatt: Wied. Ann. **38** (1899) 90, Ann. Phys. **15** (1904) 225, 425, 633.

8) P. Lenard. F. Schmidt and R. Tomaschek: *Phosphoreszenz und Fluoreszenz*, Hd. d. Exp. Phys. Vol **23** Part 1 (Akad. Verlag, Leipzig 1928) p. 327.

9) P. Lenard: Reference 8) p. 325.

* In practice, about twice of the sulphur amount required to perform the reaction (2.1) are mixed with CaO powder. The excess of sulphur is sublimated during heating.

10) W. W. Scott: *Standard Methods of Chemical Analysis* (D. Van Nostand Co. N. Y. 1939) Vol. **1**, p. 127.

Table I. Amount of SO_4^{2-}-radical in host crystal.

Flux	Amount of flux (%)	Amount of SO_4^{2-}-radical (%)
Na_2SO_4	6.00	27.2
Na_2SO_4	0.6	27.6
Na_2SO_4	0.06	26.8
K_2SO_4	0.5	26.4
KF	2.0	27.5
LiF	3.2	25.2
NaCl	2.0	25.4

pared by Lenard's method those of $CaSO_4$ crystal prepared under the same conditions are substracted, so far as the optical properties of CaS and $CaSO_4$ crystals in the host crystals are independent of one another. For this purpose, $CaSO_4$ powder crystals containing the same quantities of activator and flux as the individually prepared CaS phosphor were prepared.

3. Emission bands.

Pure host crystal consisting of CaS and $CaSO_4$ is nearly non-luminescent under 2537 Å excitation. The phosphor containing Na_2SO_4 as flux and no copper shows an emission band at about 495 mμ which increases in radiance with increasing proportion of added flux as shown in Fig. 1 a. The phosphor containing copper and no flux shown two weak emission bands at about 430 mμ and 495 mμ. When both flux and copper are added to the host crystal, the two emission bands are also observed. In general, the band at 430 mμ increases in radiance more

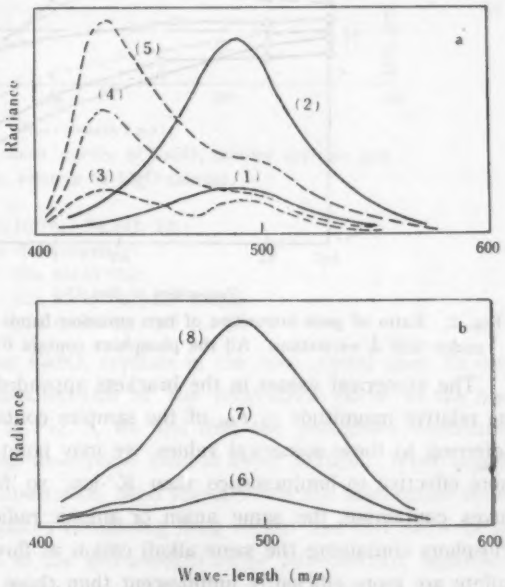

Fig. 1 a and b. Spectral-distribution curves of fluorescence of CaS phosphors, excited by 2537 Å line.
(1) Na_2SO_4 0.064%
(2) Na_2SO_4 2.000%
(3) Cu 6×10^{-3}% + NaCl 0.06%
(4) Cu 6×10^{-3}% + NaCl 0.6%
(5) Cu 6×10^{-3}% + NaCl 3.2%
(6) Cu 6×10^{-3}% + Na_2SO_4 0.064%
(7) Cu 6×10^{-3}% + Na_2SO_4 0.64%
(8) Cu 6×10^{-3}% + Na_2SO_4 3.2%

rapidly than the band at 495 mμ with increasing proportion of flux, when the flux added is a chloride (cf. Fig. 1a). On the contrary, the latter band increases in radiance more rapidly than the former with increasing proportion of flux, when a sulfate or fluoride is added as flux (cf. Fig. 1b). The ratio of peak intensity I_{430} of the band at 430 mμ to that I_{495} of the band at 495 mμ under the same excitation condition is plotted in Fig. 2 against the quantity of added flux.

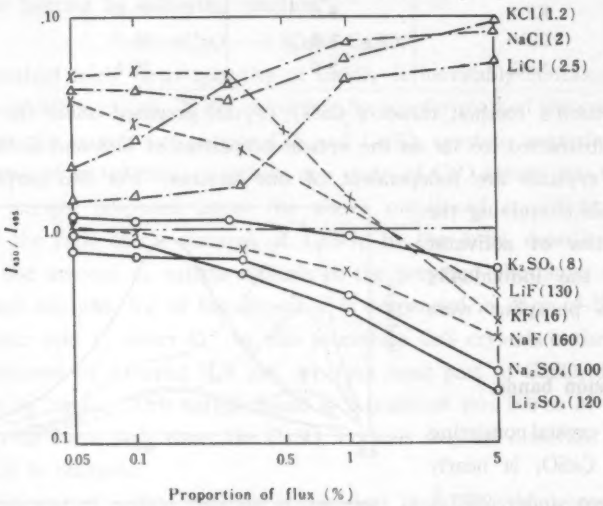

Fig. 2. Ratio of peak-intensities of two emission bands versus proportion of added flux under 2537 Å excitation. All the phosphors contain 6×10^{-3}% of Cu.

The numerical values in the brackets appended to the names of fluxes show the relative magnitude of I_{495} of the samples containing 5 weight percents of flux. Referring to these numerical values, we may point out that Na^+- and Li^+-ions are more effective to luminescence than K^+-ion, so far as the phosphors with the fluxes containing the same anion or anionic radical are concerned. Among the phosphors containing the same alkali cation as flux, those containing fluoride and sulfate are more efficiently luminescent than those containing chloride.

All $CaSO_4$ powder crystals containing copper and one of these fluxes were non-luminescent or showed only negligible luminescence. Therefore, it may be inferred that the properties stated above on the luminescence may be attributed to CaS crystals mixed in the host crystal and $CaSO_4$ crystals coexisting with them have no contribution to luminescence.

4. Ultraviolet Reflectance

Ultraviolet reflection spectra of some of the samples prepared are shown in

Fig. 3. Pure MgO powder is used as the standard of reflectance (reflectance: 100%)[11)12)]. The reflectance curves of all the prepared $CaSO_4$ powders are nearly flat over the wave-length range 240~400 mμ (Curve (1) and (2) in Fig. 3).

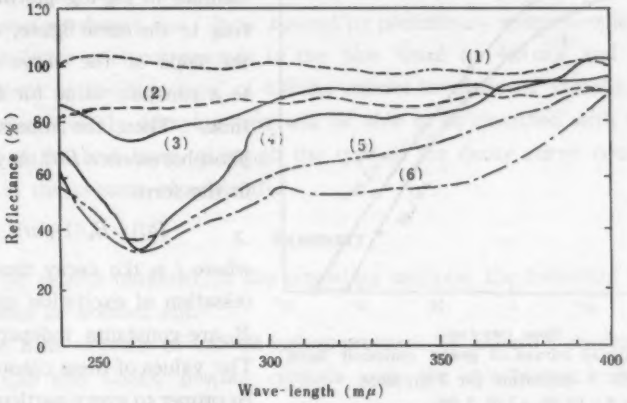

Fig. 3. Spectral-reflectance curves of $CaSO_4$ powder crystals and some CaS phosphors, relative to MgO powder.

(1) pure $CaSO_4$
(2) $CaSO_4$ (Cu 6×10^{-2}%+Na_2SO_4 2%)
(3) CaS phosphor (host-crystal)
(4) 〃 (Cu 8×10^{-2}%)
(5) 〃 (Cu 6×10^{-2}%+LiF 0.6%)
(6) 〃 (Cu 6×10^{-2}%+LiF 3.0%)

Therefore, we may infer that $CaSO_4$ crystals in the host crystal have no concern with the wave-length characteristics of the reflectance curve of the host crystal. Referring to curve (3) in Fig. 3, we find that the phosphors containing no copper and flux shows a weak absorption band at about 260 mμ. When copper is added as activator, a strong absorption band appears near the band stated above (curve (4) in Fig. 3). The phosphors containing both copper and flux show broad and nearly uniform absorption in the wave-length range 300~400 mμ, regardless of the sort of the flux added, in addition to the strong band at 260 mμ. This uniform absorption gradually increases with increasing proportion of flux, whereas the band at 260 mμ remains constant (curve (5) (6) in Fig. 3).

5. Decay of Phosphorescence

The decay of phosphorescence was measured on some of the prepared phosphors by using an electromagnetic oscillograph for early stage of the decay and

11) Jh. P. J. Botden and F. A. Kröger: Physica **15** (1949) 749.
12) S. Asano: Sci. of Light (Tokyo) **5** (1956) 66.

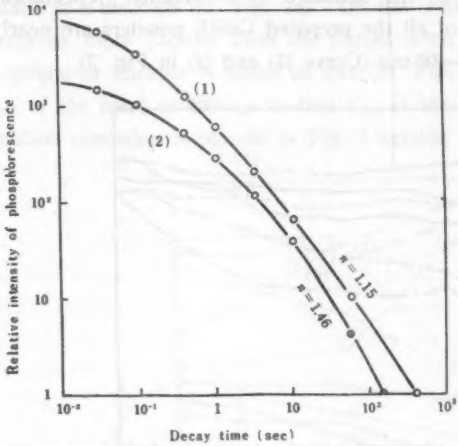

Fig. 4. Decay curves of green emission band after 2537 Å excitation for 3 minutes.
(1) Cu 6×10^{-3}%+LiF 3.0%
(2) Cu 6×10^{-3}%+Na_2SO_4 3.2%

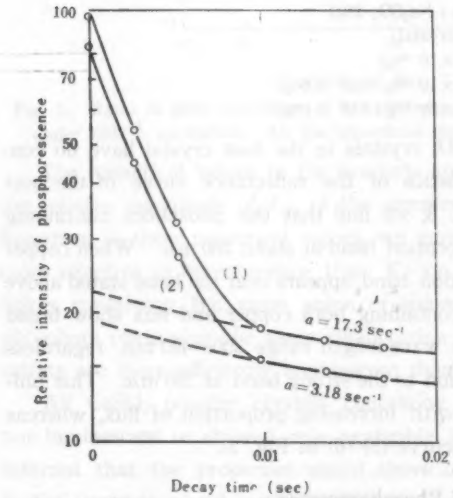

Fig. 5. Decay curuves of phosphorescence in early stage.

a sensitive galvanometer for later stage of the decay. Fig. 4 illustrates the decay curves of the prepared samples in log-log plotting. Referring to the same figure, we find that the slope of the curve approaches to a constant value for large decay time. Then the intensity of the phosphorescence $B(t)$ may be written in the form

$$B(t)=B_0/(1+at)^n, \qquad (5.1)$$

where t is the decay time after the cessation of excitation and n, a and B_0 are constants independent of t. The values of these constants should be proper to every particular sample, so far as the excitation conditions i.e. kind and intensity of excitant, duration of excitation and operating temperature are fixed constants. The values of exponent n obtained from the straight parts of the curves in Fig. 4 are also shown in the same figure. Furthermore, the aspects of the earlier stage of these decay curves are shown in Fig. 5 by semi-log plotting. The curves show conspicuous bends about 0.01 sec. after the cessation of UV excitation. The shapes of the rapidly decaying parts before the bends are indefinite, since quick following of the vibrator within 0.01 sec. was prevented by its proper frequency (150 cycles/sec.). However, we may determine fairly accurately the values of a and B_0 from the more slowly decaying parts of the decay curves in Fig. 5 and from the values of n already known. The values of a thus obtained are shown in the same figure.

If we extrapolate the slowly decaying parts in Fig. 5 towards shorter decay times by using (5.1) and the numerical values of n, a and B_0 which are determined in the above manner, we obtain the dotted curves shown in the same figure. These curves show that the phosphorescence consists of a very quickly decaying one and a long persistent one. It is assured by preliminary spectroscopic observation that the latter part corresponds to the blue band at 495 mμ and that the phosphorescence of the blue band at 430 mμ cannot be observed visually. Therefore, the former quickly decaying part will be able to be identified with the phosphorescence of the blue band, although the type of the decay curve could not be determined in the present experiments.

6. Summary

From the results obtained in the preceding sections, the following facts and inferences may be pointed ont.

(1) The host crystals of CaS phosphor prepared by Lenard's method are the mixture of CaS and $CaSO_4$ powder crystals with the stoichiometric proportion determined from the reaction (2.1).

(2) Among the main emission bands at 495 mμ and 430 mμ, the former green band will be attributed to the host crystal CaS itself, whereas the latter blue band to the copper activators in CaS crystal. (cf. Section 3)

Furthermore, the uniform absorption in the range 300~400 mμ is related with the green band and absorption at about 260 mμ with the blue band. (cf. Section 4)

(3) The sulfate and fluoride fluxes intensify mainly the green band, whereas the chloride fluxes the blue band. It should be noted that Cl^--ion is effective to the intensification of the emission band of copper in CaS crystal in a similar manner as in the case of Cu-activated ZnS phosphors[1)-4)].

(4) In general, compounds of F and Na are more effective to intensification of luminescence than those of K. It would be supposed that K^+-ion has too large ionic radius to occupy a site effective to intensification in CaS host crystal.

Solvent Effect on O-H Stretching Vibration of Methanol. I.

Yoshiki SATO

Institute for Optical Research, Tokyo University of Education
Shinjuku-ku, Tokyo

(Received Nov. 15, 1957)

Abstract

In carbon tetrachloride solutions of various oxygenated and nitrogenated organic compounds, detailed measurements of the first overtone band of methanol hydroxyl stretching vibration are made with an infrared grating spectrometer, which resulted in obtaining two new absorption bands in longer wavelengths of monomolecular OH band. Predominant behaviors are found between their intensity ratios and the basicity constants of the proton accepting molecules and also between their separations and the latter, which are explained on the basis of a potential field consisting of two minima derived in the previous paper for the motion of bonded hydrogen atom. Furthermore the feature of the potential curve is likely made clear by analyzing the above-mentioned experimental results.

1. Introduction

In the previous paper[1], it was shown that in infrared studies on the association between substituted phenols and some proton acceptors through hydrogen bond, two new absorption bands, both likely to be ascribed to the hydrogen bonding, are observed in 1.5 μ region, the appearance of which can be explained by assuming a double minimum potential for the motion of proton. Recently, measurements in 1.1 μ region for some of the above-described hydrogen bonding systems also resulted in obtaining two new absorption bands, both of which were attributed to the hydrgen bonding by considering how the potential curve for the OH valence vibration are deformed in the complexes formed by the solvent molecules with the solute molecule. Further, in a few lower levels, analogous behaviors of their wave number differences to the magnitudes of the doublet splittings of ν_2 vibration of ammonia allowed us to conclude that the height of the potential hill for proton transfer is probably about 20 Kcal./mole, for example, in hydrogen bonding between phenol and acetone[2].

In order to throw further light upon the above-mentioned idea, the examining of the dependences of intensities and separations of such two absorption bands on the basic properties of various proton acceptor molecules appears to be of

1) Y. Sato and S. Nagakura: Science of Light [Tokyo] **4** (1955) 120.
2) Y. Sato: Science of Light [Tokyo] **6** (1957) 69.

great interest, from which some informations as to the feature of the potential curve under consideration may be obtained. For this purpose, studies on the association through the hydrogen bond between methanol and several proton acceptors were made in detail by measuring the first overtone band of methanol hydroxyl stretching vibration in carbon tetrachloride solutions. As a result, close connections between the quantities in question were obtained, which led us to determine approximately the feature of the double minmum potential curve in which the proton of the associated donor molecule is in motion.

2. Experimental and Results

Methanol was used as proton donor because of its weak acidity and the well known O–H vibrational frequencies in gaseous state, and various oxygenated and nitrogenated compounds as proton acceptor. All the substances used are of special grade available, some of which were prepared by redistillations before being used. A near infrared grating spectrometer, previously described in earlier papers, was maintained at approximately constant conditions throughout this experimental work, with which all spectral measurements were made in carbon tetrachloride solutions of the proton acceptor molecules by recording spectral curves of methanol, from each of which, as the background, the absorption band of methanol itself was substracted. All of values, obtained in this way, were averaged over several runs.

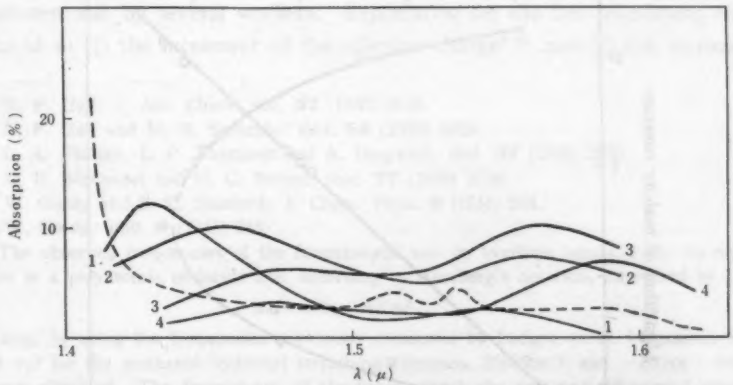

Fig. 1. Absorption curves of methanal in carbon tetrachloride solutions of: (1) 1.92 mole/l. acetophenone; (2) 2.07 mole/l. diethyl ether; (3) 1.37 mole/l. α-picoline; (4) 0.78 mole/l. tributylamine. The dotted curve is for 0.16 mole/l. methanol itself.

Some of the absorption curves obtained are shown in Fig. 1, in which two new absorption bands were found in 1.5 μ region, their shifts from the unassociated

Table 1. Relations of proton acceptors to wave numbers, separations of the two absorption bands, separations of the unperturbed levels, their shifts from the unassociated OH band, and coefficients in mixtures of zero approximation eigenfunctions.

Accepter	ν_2 (cm^{-1})	ν_1 (cm^{-1})	ΔE (cm^{-1})	i	Δ (cm^{-1})	W_{12} (cm^{-1})	Δ_1^0 (cm^{-1})	Δ_2^0 (cm^{-1})
Acetophenone	6453	7004	551	0.24	338	218	227	567
Diethyl ketone	6443	6968	525					
Ethyl acetate	6435	6951	516					
Dioxane	6431	6920	489	0.47	176	228	361	537
Diethyl ether	6421	6859	438	0.72	71	216	449	520
Quinoline	6371	6768	411	1.69	102	192	606	504
α-Picoline	6357	6768	397	1.75	112	198	618	506
Pyridine	6343	6747	405	1.84	120	193	640	520
Tributylamine	6279	6757	478	2.46	202	217	708	506
Diethylamine	6240	6772	532	2.54	231	240	734	505

OH band of methanol being listed in Table 1. As clearly seen in Fig. 1 and Table 1, the relative intensities and the separations of the two absorption bands vary characteristically with the changing of acceptor molecules. Then plotting the ratios of the maximum optical densities or extinction coefficients of the longer wavelength bands to those of the shorter ones and their separations against logarithms of the basicity constants of the acceptor molecules, Fig. 2 is obtained.

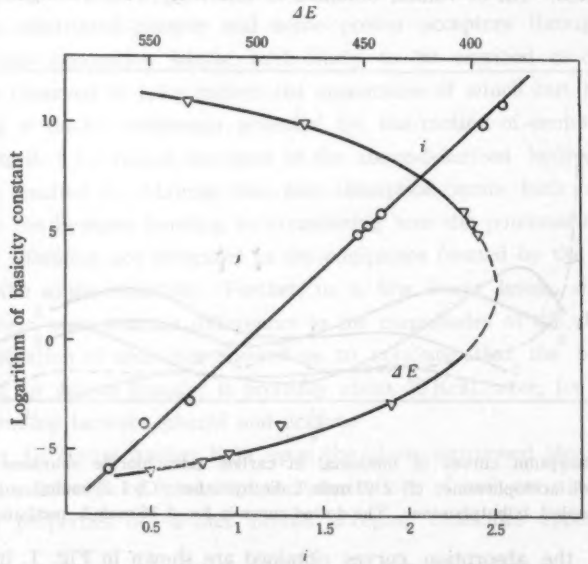

Fig. 2. Correlations of intensity ratios and separations of the two bands with the basicity constants of proton acceptors.

The basicity constants used here are the dissociation constants of the bases for water solution divided by the autoprotolysis constant of water, which were taken mainly from the data given by Hall, et al.[3)-6)]. The basicity constants for weak bases such as dioxane and diethyl ether were calculated by making use of the experimental formula given by Gordy and Stanford in their papers[7)8)].

3. Discussions

As in the case of phenol, the fact that both of the two absorption bands are related directly with the hydrogen bonding, appears no doubt from their behaviors by temperature changes of solution and concentration changes of proton acceptor, it further being cleared up by considering the deformation of the potential curve arisen from the hydrogen bond formation*. It is clearly seen in Figs. 1 and 2 that both the relative intensities and the wave number differences of the two absorption bands are closely connected with the basicity constants of the acceptor molecules. That is to say, as the base strength of the acceptor molecule increases, the longer wavelength component of the two bands decreases in intensity with the increase of the shorter one, and, at least, in the range of higher basic strengths, both of these correlations reverse. Such remarkable behaviors of the two bands can be interpreted qualitatively, on the basis of the double minimum potential previously described, as follows.

Abnormal changes of the band intensity due to the hydrogen bonding have been pointed out by several workers. Explanation for the line broadening might be reduced to (1) the increment of the effective charge[9)10)] and (2) the increase in

3) N. F. Hall: J. Am. Chem. Soc. **52** (1930) 5115.
4) N. F. Hall and M. R. Sprinkle: ibid. **54** (1932) 3469.
5) L. A. Flexser, L. P. Hammett and A. Dingwall: ibid. **57** (1935) 2130.
6) D. H. McDaniel and H. C. Brown: ibid. **77** (1956) 3756.
7) W. Gordy and S. C. Stanford: J. Chem. Phys. **9** (1941) 204.
8) W. Gordy: ibid. **9** (1941) 215.

* The observed frequencies of the fundamental and its overtone bands of the ith normal vibration in a polyatomic molecule are, according to Herzberg's notation, expressed by

$$\nu_i = \omega_i^0 v_i + x_{ii}^0 v_i^2 .$$

Calculating, by using the frequencies previously measured by Badger, et al. in gaseous state, ω_i^0 and x_{ii}^0 for the methanol hydroxyl stretching vibration, 3768 cm^{-1} and -86 cm^{-1} respectively are obtained. The frequencies of the fundamental, the first and the second overtone bands obtained in carbon tetrachloride, carbon disulfide, dichloroethylene and chloroform solutions fit in considerably well with the above equation, the corresponding potential constants in carbon tetrachloride solution, for example, being evaluated as 3726 cm^{-1} and -82 cm^{-1} respectively. In the previous cited paper[2)], these were assumed for phenol.

9) H. Tsubomura: J. Chem. Phys. **23** (1955) 2130; **24** (1956) 927.
10) G. M. Barrow: J. Phys. Chem. **59** (1955) 1129.

anharmonicity of the potential curve[11)-13)] arising from the hydrogen bonding**. If only the relative intensity of the two absorption bands is concerned, the former could be left out of our considerations. The latter is to be reduced eventually to the modifications of the eigenfunctions of ground and excited states corresponding to the infrared absorption bands under consideration, in which mixtures of eigenfunctions, which belong to the two potentials, must be superimposed in consequence of a passage through the potential barrier or tunnel effect.

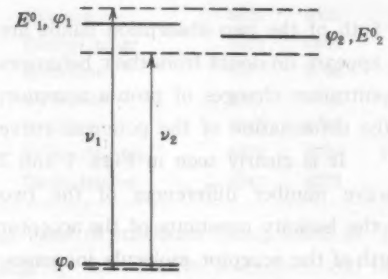

Fig. 3. Correlation of energy levels for acetophenone.

Since asymmetrical properties in double minimum potential for weak base like acetophenone seem comparatively large, relative configurations between energy levels corresponding to the two bands may be shown, for example, in Fig. 3, in which the separation of the unperturbed excited levels is not very large as described below. In consequence of the perturbation, the vibrationless eigenfunction can be shown to be $\Psi_0 (\simeq \varphi_0)$, and also the perturbed excited eigenfunctions to be the following mixtures of the zeroapproximation eigenfunctions:

$$\begin{aligned} \Psi_{II} &= a\varphi_1 + b\varphi_2 \\ \Psi_I &= a\varphi_2 - b\varphi_1, \end{aligned} \tag{1}$$

where the coefficients a and b are determined as functions of the perturbation energy W_{12} and the separation of the unperturbed levels, Δ, as follows:

$$\begin{aligned} a &= (\sqrt{4|W_{12}|^2+\Delta^2} - \Delta/2\sqrt{4|W_{12}|^2+\Delta^2})^{1/2} \\ b &= (\sqrt{4|W_{12}|^2+\Delta^2} + \Delta/2\sqrt{4|W_{12}|^2+\Delta^2})^{1/2}. \end{aligned} \tag{2}$$

The perturbed level E is given by

$$E = \frac{1}{2}(E^0_1 + E^0_2) \pm \frac{1}{2}\sqrt{4|W_{12}|^2+\Delta^2} \tag{3}$$

Then the difference between the energies of the resulting two states is expressed by

$$\Delta E = \sqrt{4|W_{12}|^2+\Delta^2}. \tag{4}$$

From Eq. (1), the matrix elements of the transition moments corresponding to the two absorption bands are calculated as

11) R. H. Badger and S. H. Bauer: J. Chem. Phys. **5** (1937).
12) M. Davis and B. M. Sutherland: ibid. **6** (1938) 755.
13) H. L. Frisch and G. L. Vidale: ibid. **25** (1956) 982.

** The spectral complexity may also be considered as resulting from molecules having various degrees of polymerization. See, for example, Cross, Burnham and Leighton: J. Chem. Soc. 59 (1937) 1134; R. Mecke: Disc. Farady Soc. **9** (1950) 161.
This line broadening will be further discussed in later paper.

$$M_{0I}=\int\Psi_I^*\boldsymbol{M}\Psi_0 d\tau\simeq a\int\varphi_2^*\boldsymbol{M}\varphi_0 d\tau-b\int\varphi_1^*\boldsymbol{M}\varphi_0 d\tau$$
$$M_{0II}=\int\Psi_{II}^*\boldsymbol{M}\Psi_0 d\tau\simeq a\int\varphi_1^*\boldsymbol{M}\varphi_1 d\tau+b\int\varphi_2^*\boldsymbol{M}\varphi_0 d\tau\,. \qquad (5)$$

Under the conditions $b>a$, which is obtained from Eq. (2), and $\int\varphi_1^*\boldsymbol{M}\varphi_0 d\tau>\int\varphi_2^*\boldsymbol{M}\varphi_0 d\tau$, which may easily be understood from the overlapping between the eigenfunctions, $M_{0I}>M_{0II}$, which requires, as shown by the experimental fact, the intensity of the shorter wavelength band to be larger than that of the longer wavelength band.

The basicity constant is considered as a measure of proton attracting power (Broensted base). As this constant of the proton acceptor molecule increases, it is to be expected that both the zero-order frequency and the anharmonicity constants for the first potential increases, which correspond to elongation of the OH bond length, and that the minimum of the second potential, on the other hand, is lowered with the increment in the zero-order frequency. As a consequence, the unperturbed energy levels approach each other, which would be followed by the reversal of their relative configurations. That is satisfactorily inferred from the fact that, with the increase of the basicity constant of the acceptor molecule, both of the two absorption bands shift toward the longer wavelengths and the magnitude of their saparation becomes minimum at an intermedate basic strength, as shown in Fig. 2. The above-mentioned facts are discussed somewhat quantitatively in the following.

Concerning the band intensity and from Eq. (4), it is very desirable to measure integrated extinction coefficients rather than extinction coefficients of band maxima, the former necessitating a correction for finite slit width to be made which is very small in an instruments with a large resolving power. If the feature of the observed absorption bands follows the Lorentz curve, $a/(\nu-\nu_0)^2+b^2$, in the case in which the difference in the half-widths seems unlikely large, the former is possible to be replaced approximately by the latter, since the integrated and maximum extinction coefficients are given by $\pi a/clb$ and a/clb respectively[14].

Neglecting the matrix element $\int\varphi_2^*\boldsymbol{M}\varphi_0 d\tau$ in Eq. (5), the intensity ratio is given by

$$i\approx b^2/a^2=(\sqrt{4|W_{12}|^2+\Delta^2}+\Delta)/(\sqrt{4|W_{12}|^2+\Delta^2}-\Delta)=(\Delta E+\Delta)/(\Delta E-\Delta)\,. \qquad (6)$$

The separations of the unperturbed levels, Δ, are therefore evaluated using the values of i and ΔE determined experimentally with the aid of Eq. (6), followed by

14) D. A. Ramsay: J. Am. Chem. Soc. **74** (1952) 72.

calculation of the corresponding perturbation energies W_{12} from Eq. (3) shown in Table 1. Furthermore, the values of the coefficient b which are obtained from Eq. (2), and the shifts of the unperturbed levels which are calculated by the use of Eq. (5) from the original level corresponding to the unassociated band, Δ_1^0 and Δ_2^0, are also listed in the same table. In Fig. 4, Δ, Δ_1^0, Δ_2^0 and b are plotted respectively against the basicity constants of the acceptor molecules. As seen in the figure, minimum value of Δ is probably situated at the basicity constant with which the relative intensity of the two absorption bands becomes equal to one, which is in good agreement with what is likely to be expected from Eqs. (2) and (3). In addition, for weak base such as nitrobenzene, the basicity constant of which is about -10, the value of b is almost equal to one, which results in disappearing of longer wavelength one of the two absorption band agreeing well with the experimental fact. The perturbation energies are all approximately constant, which also to be anticipated qualitatively, and their values appear reasonable as compared with the value of 157 cm^{-1} for the doublet splitting of $2\nu_2$ vibration of ammonia. Moreover, it is of interest to note that while Δ_1^0 considerably varies with the basicity constant of the acceptor molecule, Δ_2^0 remains approximately constant.

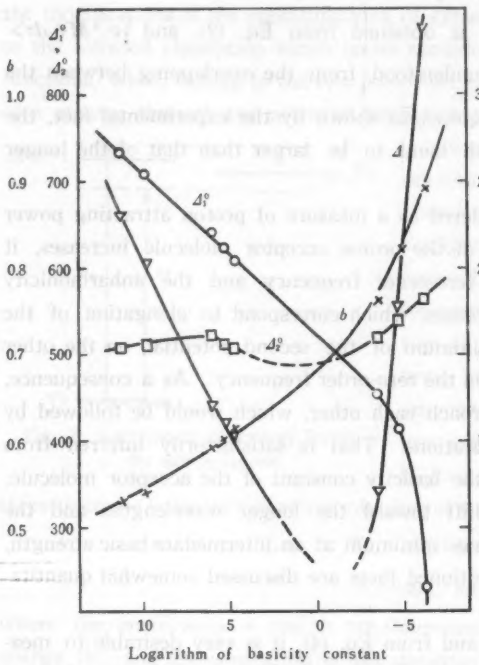

Fig. 4. Correlations of Δ, Δ_1^0, Δ_2^0 and b with the basicity constants of proton acceptors.

Thus the remarkable behaviors of the intensities and the separations of the two absorption bands related with the changing of basic properties of the proton acceptor molecules could be understood by the deforming of the double minimum potential. Furthermore, the feature of the potential curve could almost be determined in combination with the data which are obtained from measurements of the fundamental and the first overtone regions and by analysis similar to the above.

Finally, let us discuss the dependence of the frequency shift on the hydrogen bond energy. It seems reasonable to consider the value of Δ described above as a measure of the strength of the hydrogen bond. In fact, Δ monotonically varies with the changing of the basicity constant of the proton acceptor molecule, as seen in Fig. 4, and, in the case in which it can be regarded that only a single absorption band results from hydrogen bonding, its shift from unassociated absoption band has usually been considered as a measure of the strength of the hydrogen bond. In Fig. 5, the average value, δ, of the shifts of the two absorption bands from the free OH band, which is obtained from only the experimental work, is plotted against Δ. The linear relation between them as seen in the figure shows that the relative strength of the hydrogen bond can be inferred from the magnitude of the former. It is important to note that, as clearly seen in the figure, the order of hydrogen bonding strengths of the acceptor molecules is reverse to that expected from the magnitude of their dipole moments, whereas it is parallel to that expected from the magnitude of their ionization potentials, as mentioned in the previous paper[1].

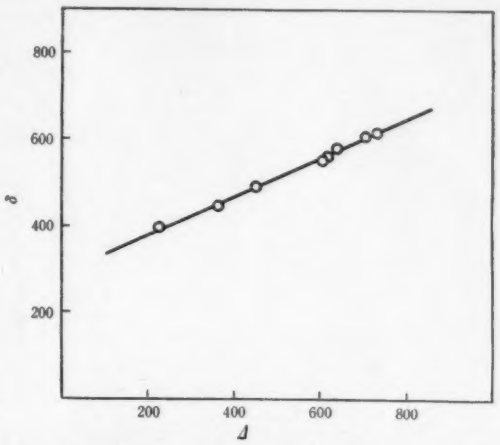

Fig. 5. Relation of average values of the shifts of the two absorption bands to Δ's.

Aknowledgements

The author sincerely thanks to Professors Y. Fujioka and H. Ootsuka for their deep interest and encouragement, to Professor M. Seya for his valuable comments and to Dr. S. Nagakura for his advice. He is grateful to Asst. Professor S. Hachisu and his co-workers for their facilities offered in purification of the samples.

17318